HIGH SPEED IMAGING INVESTIGATIONS OF THE PLASMA PLUME DURING DIRECTED ENERGY DEPOSITION ADDITIVE MANUFACTURING

Robert RADU[1], Sabin MIHAI[2], Diana CHIOIBASU[3], Andrei C. POPESCU[4] and Cristina STAN[5, *]

In this paper we present a study on the spatio-temporal evolution of the plasma plume during directed energy deposition additive manufacturing of a metal matrix composite consisting of a nickel alloy IN718 (INCONEL) with a dispersed phase in form of TiC (titanium carbide) particles at different concentrations. The images of the plume area recorded with high-speed camera and postprocessed in data sequences were analyzed using power spectral density and multifractal detrended analysis of the fluctuations. This type of investigation can predict based on associations with results from other methods of investigation the quality of the deposition, the eventual presence of defects or the metallographic microstructure.

Keywords: Directed Energy Deposition, area plume, power spectral density, multifractal analysis

1. Introduction

Directed Energy Deposition (DED) [1,2] is an additive manufacturing process that can be used to produce Metal Matrix Composites - MMC materials in situ. Using this technique, mixed metal-ceramic powders with known compositions are molten by a laser beam and solidify upon the cease of the beam's action into a composite material [3,4]. An extensive study on the manufacturing synthesis of Titanium Metal Matrix Composites—TMC with a dispersed phase of TiC by

* Corresponding author
[1] PhD student, Faculty of Applied Sciences, UNSTPB Bucharest, Romania, e-mail: radurobert@yahoo.com
[2] Development Engineer III, National Institute for Laser, Plasma and Radiation Physics, Magurele, Romania, e-mail: sabin.mihai@inflpr.ro
[3] Development Engineer I at National Institute for Laser, Plasma and Radiation Physics, Magurele, Romania, e-mail: diana.chioibasu@inflpr.ro
[4] Scientific Researcher I at National Institute for Laser, Plasma and Radiation Physics, Magurele, Romania, e-mail: andrei.popescu@inflpr.ro
[5,*]Prof., Faculty of Applied Sciences, UNSTPB Bucharest, Romania, e-mail: cristina.stan@upb.ro

directed energy deposition was presented in [5], with the investigations focused on the effect of TiC content on the phase evolution of the titanium. Thus, the TiC content improved the mechanical properties such as hardness, tensile strength, and wear resistance in the TMC composite. According to the analyses of the metallographic morphologies of TMCs with different TiC content, the TiC powders concentrations could significantly influence the melting and dissolution processes involved in metal deposition.

A great interest for experimentalists is to develop methods to identify defects and element agglomerations occurring during the additive manufacturing of metallic matrix composites. A novel method of nondestructive characterization via X-ray and high-speed imaging of IN718/TiC composite materials manufactured by DED was reported in [6]. The authors developed a method that correlates the molten pool's area and temperature during DED with the evolution of the microstructure and metallographic phases. To link defects and particle agglomerations possible in the additive manufacturing of metallic matrix composites, the authors used high-speed camera images and X-Ray microtomography. In [6] it was reported that the width of the deposited samples was correlated with the fluctuation of the melt pool area recorded by high-speed imaging.

Methods based on multifractal analysis are considered powerful tools for characterizing complex systems, irrespective of their number of components or types of interactions at different times or spatial scaling [7-11]. In addition to classical statistical analysis that provides information on the global properties of stationary data (mean, variance, etc.), new insights can be obtained particularly when dealing with complex, non-uniform data, without prior knowledge of their underlying structure.

In the domain of quality control and Materials Science, the mechanical properties such as surface roughness, fracture patterns, and other material properties often exhibit multifractal scaling. Usually, multifractal analysis was performed on the TEM or AFM images of thin film morphologies [12-16]. For instance, a multifractal approach for diamond-like carbon (DLC) deposited by pulsed laser deposition (PLD) technique at different substrate temperatures was reported by [14]. A quantitative dependence between the parameters of the multifractal spectrum of the surface microforms formed during the face milling of samples in different experimental conditions was proposed in [15] together with a three-dimensional fractal model specifically designed for morphological analysis.

In this paper, we propose a study on the correlations presented in the spatio-temporal dynamics of plasma plume formed during the laser melting deposition in the manufacturing synthesis of nickel alloy metal matrix IN718 and a dispersed phase in form of TiC particles at different concentration using the multifractal analysis of plume area. Based on the fragmentation of the time series in self-similar segments investigated in relation with the scaling properties derived from a power

law behavior, such analysis can detect and quantify the fluctuations intensity at different scale range, extreme events and singularities and can capture the hidden dynamics generated by short or long-range correlations. In this way, it is possible to link the fluctuations in plume area formed during DED processing of IN718/TiC composite and singularities, defects or unexpected properties of the deposited MMC.

The structure of the paper is as follows: the experimental methodology, data analysis and MFDFA are presented in section 2. The results obtained for different environments and the analysis of multifractality are presented in section 3, while the main conclusions of the article are summarized in section 4.

2. Experimental and theoretical methods

In order to investigate the plasma plume generated during the DED process of a metal matrix composite based on IN718 nickel alloy with dispersed TiC particles at various concentrations, an automated robotic system (Kuka, Augsburg, Germany) was employed. The robot was equipped with an optical fiber for laser beam delivery and two powder feeding nozzles for IN718 and TiC. The process used a continuous-wave Yb:YAG disk laser (Trumpf, Ditzingen, Germany) set to a power of 1.1 kW, with a spot diameter of 0.8 mm and an infrared wavelength of 1030 nm. To ensure uniform delivery of the powders onto a 304 stainless steel substrate, a shielding and carrier gas mixture of helium and argon was used to transport the powders into the laser beam focal zone from a powder feeder device with two vessels for powder storage, one filled with IN718 and another with TiC.

Figure 1 shows a schematic view of the experimental arrangement.

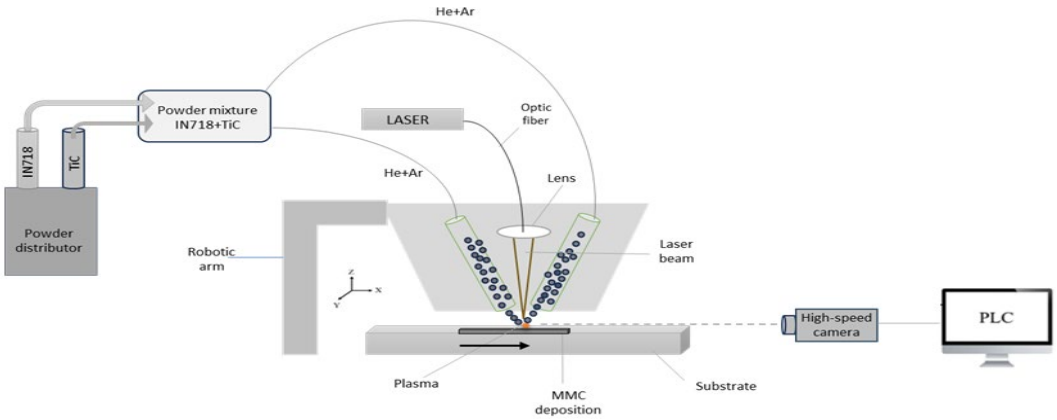

Fig.1 Schematic experimental setup for obtaining MMC through the DED technique

The analysis presented in this paper is based on the data analysis of the plasma plume images in their spatio-temporal evolution during the deposition

process. Four distinct experiments of deposition of composites are considered: IN718, IN718+5%TiC, IN718+10%TiC and IN718+15%TiC.

The images of the plasma plumes have been recorded at different times during the deposition, using a high-speed camera CMOS, Mini AX100 (Photron, Tokyo, Japan), with 32GB internal memory with 50 mm focal distance NIKKOR lens, arranged parallel to the surface of the MMC depositing at 380mm. The selected resolution was 384 × 384px at 13.600 fps with an exposure time of 1/fps for recording the process of tracing a 20-22 mm line by DED. To attenuate the laser radiation, a 5.5 mm neutral density filter and a colored filter RG610 were used.

Some typical plasma images are shown in Fig.2.

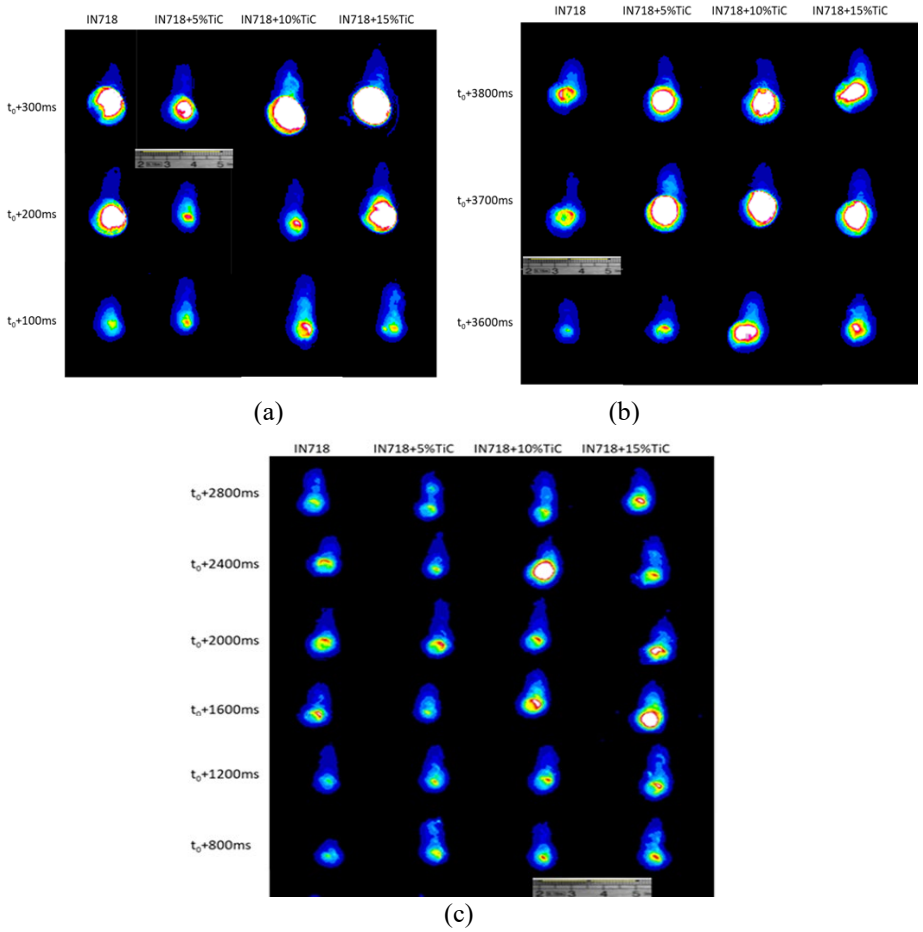

Fig. 1 Spatio-temporal evolution of representative plasma plume recordings for each investigated material deposition in three distinct regimes (a) first stage (0-300ms), (b) final stage (3600-3800ms), (c) quasi-stationarity (between).

The plasma cloud resulting from DED process has the shape of a plume with varying area depending on the TiC addition. The plasma plume emerges from the substrate. The representative high-speed images in Fig.2 are arranged in three

different groups corresponding to the three distinct regimes that can be easily identified. During the deposition process, large area plumes have been observed at the beginning (Fig.2a) and at the end (Fig.2b) of the process and smaller plume areas in the interval between (Fig.2c). These regimes were also observed in the case of metallographic spatial deposition as reported in [6].

In the quasi-stationary regime, for pure IN718, the plasma appears compact and centrally concentrated, with no evident lateral extensions. With the addition of 5% TiC, the plume becomes slightly elliptical, showing more diffuse edges compared to pure IN718. At higher concentration of TiC the plasma plume becomes wider, more intense, and better defined, with increasingly larger areas favoring energy absorption and the formation of an extended liquid phase.

Using the open-source software ImageJ (LOCI, University of Winsconsin, Madison, WI, USA), postprocessing operations of cropping and binarization of pictures were made to determine the areas of plasma plumes. Data sets for each concentration of TiC are considered as distinct sequence imprinting information related to the intrinsic space-time dynamics in the particular interaction laser-powder.

Figure 3 gives the evolution of plasma area dynamics for each of the considered sample cases. The three regimes of different ranges of plasma area are obviously evidenced in the values of the measured area plume (large mean values at the beginning and at the end and smaller values in between time deposition.)

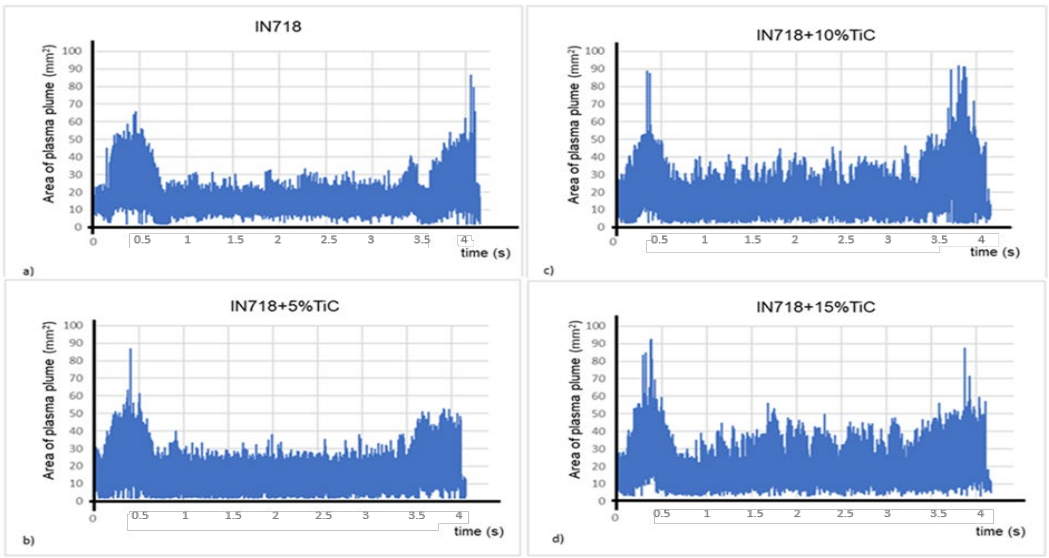

Fig. 3 Graph of plasma area variation for the four samples: a) IN718, b) IN718+5%TiC, c) IN718+10%TiC, IN718+15%TiC

The data sets for each TiC concentration for the quasi-stationary regime are shown in Fig.4, together with the corresponding power spectral density of the detrended data (mean values removed).

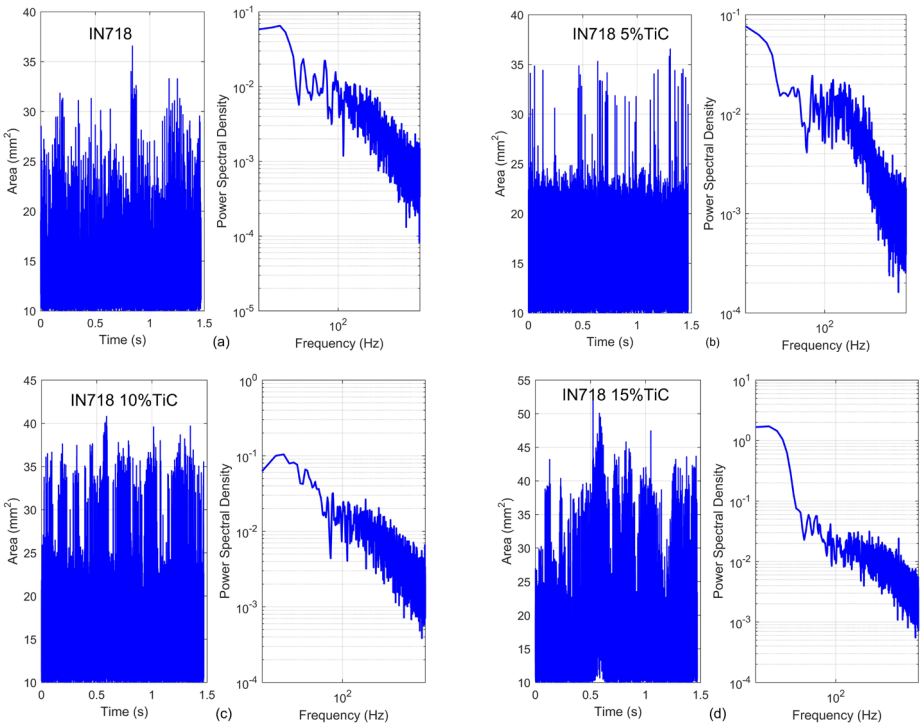

Fig. 4 Plume area evolution in the quasi-uniform regime of deposition and the corresponding power spectral density for the four samples: a) IN718, b) IN718+5%TiC, c) IN718+10%TiC, d) IN718+15%TiC

For each of the deposition cases, the power spectral density shows the same type of power law dependence but with different slopes.

In performing the multifractal detrended fluctuation analysis (MF-DFA), we consider data sets of 20000 points taken in the same time interval, after a reasonable start and enough before the stopping times of laser operation.

The problem of how to distinguish between the temporal variation of the plume area in DED of MMC for different TiC concentrations can be analyzed based on multifractal formalism. Specific multifractal spectra of the time-series fluctuations observed in the areas of the luminous plasma plumes formed as the results of interaction between laser and powder composite can give complementary information on the quality of the final deposition properties.

Multifractal Detrended Fluctuation Analysis (MF-DFA) involves the computation of the q-order local fluctuation function $F(q,s)$ from profile series of N points after the best polynomial fit on specific segments ν =1, 2, …, N_s=Int(N/s) of size s as [7,17]:

$$F(q,s) = [\frac{1}{2N_s} \sum_{k=1}^{2N_s} \{[F^2(\nu,s)]^{\frac{q}{2}}\}^{\frac{1}{q}} \quad (1)$$

where $F^2(\nu,s)$ is the variance on interval s [7]. The negative values of the q-order fluctuation functions emphasize larger fluctuations, making it sensitive to periods with high variability in the data and the positive values ($q > 0$) data demonstrate smaller fluctuations, focusing on periods with low variability.

In the case of a statistically self-affine series, the dependence of the fluctuation function on the size s of the segment is expected to be power law type:

$$F(q,s) \approx s^{H(q)} \quad (2)$$

where $H(q)$ is known as the generalized Hurst exponent which represents the measure of the correlations in the fluctuations of the series. Obviously, this can be computed from the log–log plot of the fluctuation function vs. s, as the slope in the scaling region. If $H(q) > 0.5$ the correlations in the time series are persistent, i.e. an increment has higher probability of being followed by another increment. Conversely, if $H(q) < 0.5$ the correlations in the time series are antipersistent, i.e. an increment has more chances of being followed by a decrement. Non-correlated data set specific for Gaussian white noise corresponds to a constant value $H(q)$ =0.5 [9].

The singularity spectrum is described by the curve:

$$f(\alpha) = q\alpha - \tau(q) \quad (3)$$

where the $\tau(q)$ and α are defined as:

$$\tau(q) = qH(q) - 1 \quad (4)$$

$$\propto = d\tau(q)/dq\,. \quad (5)$$

The singularity spectrum gives information on the distribution of the dimensions $f(\alpha)$ of subsets of the series characterized by various values of the singularity strength α. It describes the irregularity or heterogeneity of the system dynamics across different scales. If α =1, the distribution of the data is uniform, similar to a gaussian noise, and larger/smaller interval of values of α evidence smaller/larger singularity degree in the data sets.

The multifractal spectrum is usually quantified by the position of the maximum ($\propto_{\max}$), the width of the spectrum (singularity interval) $\Delta\alpha = \propto_{\max} - \propto_{\min}$ and by the difference in fractal dimensions $\Delta f = f(\propto_{\max}) - f(\propto_{\min})$.

3. Results

Figure 5 presents the fluctuation functions, Hurst exponent and singularity spectrum for the four data sets of the area plume in the cases of deposition of composites of IN718, IN718+5%TiC, IN718+10%TiC and IN718+15%TiC.

The formalism of MFDFA and all the computations were implemented and computed using Mathematica software. As observed in the first line of Fig.3, the fluctuation functions in all the studied cases show a power law dependence demonstrating the properties of self-similarity. We chose for s the interval (40-400) in looking for the dynamics involved in the short and medium time scale around (3-30) ms, where laser influence and thermal diffusion are dominant. Values of s<40 determine an arithmetic underflow. Different slopes in the $F_q(q)$ or cross-overs in the graphs indicate different regimes characterized by different scaling behavior.

Based on the logarithm of fluctuation functions versus log(s) for different values of q we get the values of Hurst exponents, represented in the second line of Fig.5. The continues curves superposed on the red points are the best fitted logistic functions usually used for the estimation of the values of H(0) which is directly related to the box-counting dimension (H(q=0) = D – 1, where D is the fractal or capacity dimension) [12, 18, 19].

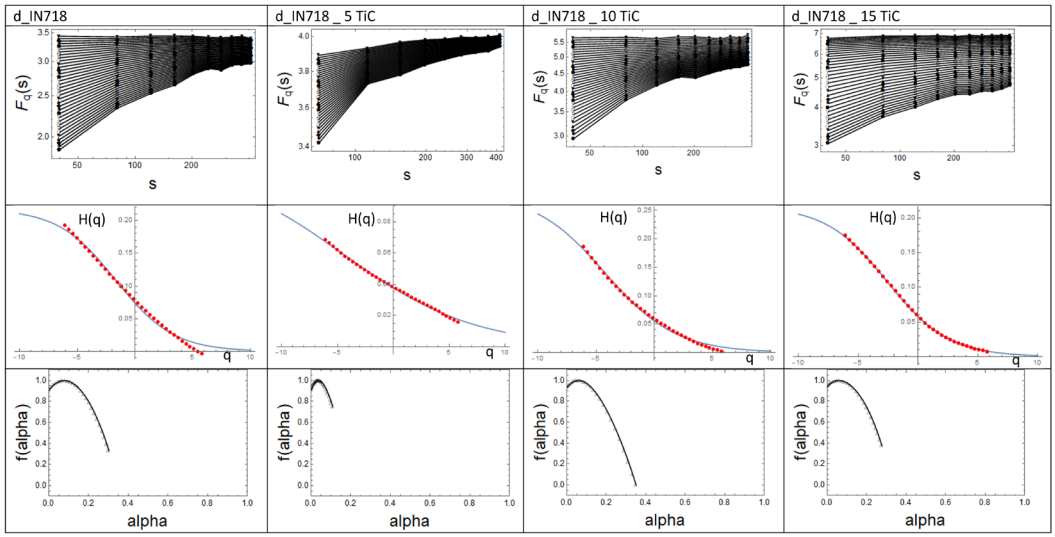

Fig. 5 Fluctuation functions (first line), Hurst exponents (second line) and singularity spectrum (third line) for the analyzed TiC composites

All the values of the Hurst exponents are below 0.5 meaning that all the data sets have the same anti-persistent or anti-correlated type behavior. Consequently, the dynamics involved in all the cases in this time scale range is characteristic to processes tending to reverse direction. If at a specific moment the value has been

increasing, they are more likely to decrease in the next, and vice versa. This creates a "mean-reverting" character which is similar at both large and slow fluctuations scales.

The truncated shape and the asymmetry of the singularity spectrum signifies the absence of regions with high regularity in all the investigated cases.

The overall resemblance of the results for all the studied cases indicates a similar evolution controlled by the same type of dynamics involved in laser-powder interaction during the deposition process. However, there are specific differences in the values of the multifractal parameters for the data sets of area plume for different powder concentration. The values that quantify the curves from the second and third lines are summarized in Table 1.

Table 1

Strengths of multifractality

	H(q=0)	$\Delta\alpha$	α_{max}	Δf
D_IN718	0.072	0.31	0.08	0.58
D_IN718_5TiC	0.037	0.11	0.04	0.16
D_IN718_10TiC	0.054	0.35	0.06	0.95
D_IN718_15TiC	0.059	0.28	0.06	0.58

Theoretically, it is well known that the singularity spectra at the minimum value of α indicates the maximum fluctuation of the data which, in our investigations seems to be similar in each case, but the strength of singularity indicates a range of small and large fluctuation specific for a certain concentration of TiC. The lowest values for almost all the multifractal parameters are observed for the data corresponding to D_IN718_5TiC. A small value for Δf demonstrates insignificant proportion of the small and large peak values of the fluctuation, therefore a much more stable dynamics than for the rest of the situation. Since the larger $\Delta\alpha$ means the larger the multifractal characteristics scale and complexity of the time series data with large fluctuations, the case of 5%TiC shows again a particular characteristic with relatively small fluctuations and inhomogeneity of the distribution, much lower than for the other TiC powder concentration.

A shuffling of the data sets of area fluctuations for each sample destroys all the small-range correlations. The computed singularity spectra for each case of our investigation does not change the shape after this procedure, demonstrating that the source of multifractality is caused both by long-range correlation between small and large fluctuations [9].

As an overall conclusion of the whole processes involved during direct energy deposition additive manufacturing of metal matrix composite of a nickel alloy IN718 (INCONEL) with a dispersed phase in form of TiC particles, we can summarize the following. At the beginning and the end of the DED process, the

temperature is higher, due to a short stationary period of the robotic arm after the laser starts and a slow down at the end of the process, before the laser turns off. This also translates into a larger and brighter plasma plume. Between these maxima of the plume areas, the plume intensity varies slightly during the entire deposition process. From the fractal analysis it can be observed that the increasing addition of TiC particles in the process causes more fluctuations of the plume intensity and area, with characteristic multifractal spectra. This is probably due to an absorption of the laser beam by the TiC particles inserted in the molten pool, which increases the melting point of the MMC and destabilizes the melt pool. Moreover, the more TiC particles expulsed through the nozzle channels, the more different the laser absorption will be before they reach the molten pool. While we try to ensure a steady flow of powders, it is no guarantee of a linear flow of powders through the hoses and nozzle, the flow variations causing plume intensity and size variation.

4. Conclusions

In this paper we present investigation on the spatio-temporal dynamics of plasma plumes generated during the process of Directed Energy Deposition. The luminous plumes were recorded using a high-speed camera and then postprocessed with ImageJ for computing the plume areas at equal time intervals during the deposition. We performed a multifractal analysis of data sets sequences of area fluctuations in the space-time domain of practical interest, for different concentrations of TiC powder into the IN718 matrix.

Our results show values of the Hurst exponents below 0.5 characteristic to an anti-correlated dynamics of laser-powder and specific multifractal characteristics for the four distinct experiments of deposition of composites IN718, IN718+5%TiC, IN718+10%TiC and IN718+15%TiC.

The results of MFDFA show that the most stable dynamics with small proportion of small and large peak correspond to wt.% 5TiC, which is in good agreement with the experimental measurements [5,6] that confirm this concentration as a better choice for a good quality in the additive manufacturing. It also be considered as additional support in demonstrating that the instability and fluctuation of plasma plume area reflect possible defects in the process of deposition and in mechanical properties.

The multifractal analysis of the plume area offers useful information related to the complexity of the dynamics hidden at the fluctuation levels and can predict in synergy with other methods of investigation the quality of the metallographic phases in DED. Also, this type of analysis can be corroborated with the results of a multifractal analysis of the surface topography to give good prediction on the quality of the resulted material and to optimize the working parameters in the deposition processes. In this way, in our opinion, such investigations on the spatial-

temporal plume area could be useful as possible tools for a primary adjustment of the working parameters such as laser power, scanning speed and powder flow rate and concentration, for achieving an optimal multifractal profile associated with a superior deposition quality. Further studies are planned for a deeper investigation of the cross-correlation between the temperature of the plume and its dimension and, also with the surface morphology in connection with the mechanical properties of the deposition for different concentration of the TiC powder into the IN718 matrix.

Acknowledgement

Part of this work was supported by the Romanian Ministry of Research, Innovation, and Digitalization under Romanian National Core Program LAPLAS VII-contract no. 30N/2023. We also acknowledge the support of National Interest Infrastructure facility IOSIN – CETAL at INFLPR.

REFERENCES

[1] *A. Saboori, D. Gallo, S. Biamino, P. Fino, M. Lombardi*, An overview of additive manufacturing of titanium components by directed energy deposition: microstructure and mechanical properties, Applied Science, Vol. **7**, Iss. 9, 2017.

[2] *M.A. Mahmood, A.C. Popescu, I.N. Mihailescu,* Metal matrix composites synthesized by laser-melting deposition: a review. Materials, Vol. **13**, Iss. 11, 2020.

[3] *J. Elambasseril, J. Rogers, C. Wallbrink, D. Munk, M. Leary, M. Qian,* Laser powder bed fusion additive manufacturing (LPBF-AM): the influence of design features and LPBF variables on surface topography and effect on fatigue properties, Critical Reviews in Solid State and Material Sciences, Vol. **48**, Iss. 1, 132-168, 2023.

[4] *S.R. Narasimharaju, W. Zeng, T.L. See, Z. Zhu, P. Scott, X. Jiang, S. Lou,* A comprehensive review on laser powder bed fusion of steels: processing, microstructure, defects and control methods, mechanical properties, current challenges and future trends, Journal of Manufacturing Processes, Vol.**75**, 375-414, 2022.

[5] *S. Mihai, F. Baciu, R. Radu, D. Chioibasu, A.C. Popescu,* In situ fabrication of TiC/Ti–matrix composites by laser directed energy deposition, Materials, Vol. **17**, Iss. 17, 2024.

[6] *S. Mihai, P. V. Toma, A. Sima, D. Chioibasu, A.C. Popescu,* A novel method of nondestructive characterization via X-ray and high-speed imaging of TiC/IN718 composite materials manufactured by LMD. Results in Engineering, Vol. **24**, Iss. 4, 2024.

[7] *J.W. Kantelhardt, S.A. Zschiegner, E. Koscielny-Bunde, S. Havlin, A. Bunde, H.E. Stanley,* Multifractal detrended fluctuation analysis of nonstationary time series, Physica A: Statistical Mechanics and its Applications, Vol **316**, Iss. 1-4, 87–114, 2002.

[8] *S. Vahab, A. Sankaran,* Multifractal applications in hydro-climatology: a comprehensive review of modern methods, Fractal and Fractional, Vol. **9**, Iss. 1, 2025.

[9] *C. Stan, C. M. Cristescu, D. Alexandroaei, C.P. Cristescu*, The effect of Gaussian white noise on the fractality of fluctuations in the plasma of a symmetrical discharge, Chaos, Solitons & Fractals Vol **61**, 46–55. 2014.

[10] *E.I. Scarlat, C. Stan, C. P. Cristescu,* Chaotic features in Romanian transition economy as reflected onto the currency exchange rate, Chaos, Solitons & Fractals, Vol **33**, Iss. 2, 2007, 396-404.

[11] *X. Zhang, G. Zhang, L. Qiu, B. Zhang, Y. Sun, Z. Gui, Q. Zhang,* A modified multifractal detrended fluctuation analysis (MFDFA) approach for multifractal analysis of precipitation in Dongting Lake Basin, China, Water, Vol .**11**, Iss. 5, 2019.

[12] *C. Stan, M. Balasoiu, A.I. Ivankov, C.P. Cristescu,* Multifractal analysis of CoFe2O4/2DBS/H2O ferrofluid from tem and sans measurements, Romanian Reports in Physics, Vol. **68**, Iss.1, 270-277, 2016.

[13] *Z. Chen, J. Lai, C. Shek,* Multifractal spectra of scanning electron microscope images of SnO2 thin films prepared by pulsed laser deposition, Physics Letters A, Vol. **345**, Iss. 1-3*,* 218-223, 2005. [14] *A. Modabberasl, M. Sharifi, F. Shahbazi, P. Kameli,* Applied Surface Science, Vol. **479**, 639-645, 2019.

[15] *M.A. Mahmood, K. Ishfaq, M. Sana, S. Anwar,* 3D fractal model with experimental analysis for assessing surface topography in EDM, Surface Topography: Metrology and Properties, Vol. **12**, Iss. 2, 2024.

[16] *N. Balytska, L. Penter, V. Kryzhanivskyy, O. Melnyk, L. Polonsky, V. Shadura, S. Ihlenefldt, P. Moskvin*, Multifractal parameterization of a periodic surface microrelief formed at the face milling. 2. Distribution of elements volume of surface relief, Multiscale and Multidisciplinary Modeling, Experiments and Design, Vol. **7**, 1781–1791, 2024.

[17] *C.K. Peng, S.V. Buldyrev, S. Havlin, M. Simons, H. E. Stanley, A. L. Goldberger,* Mosaic organization of DNA nucleotides, Physical Review E, Vol. **49**, Iss. 2, 1994, 1685–1689.

[18] *C. Stan, L. Marmureanu, C. Marin, C.P. Cristescu*, Investigation of multifractal cross-correlation surfaces of Hurst exponents for some atmospheric pollutants. Physica A: Statistical Mechanics and its Applications, Vol **545**, 2020.

[19] *C. Marin, C., Stan, C., & Cristescu, C. P. (2021).* Multifractal cross-correlation of atmospheric pollutants and temperature in different environments, UPB Sci. Bull., Series A, Vol. **83**, Iss.2, 227-238, 2021.